JOURNAL OF SOLID STATE CHEMISTRY **138,** 201–206 (1998)
ARTICLE NO. SC987772

Magnetic and Electrical Properties of a New Series of Rare Earth Silicide Carbides with the Composition $R_3Si_2C_2$ (R = Y, La–Nd, Sm, Gd–Tm)

Martin H. Gerdes, Anne M. Witte, Wolfgang Jeitschko,[1] Arne Lang, and Bernd Künnen

Anorganisch-Chemisches Institut, Universität Münster, Wilhelm-Klemm-Straße 8, D-48149 Münster, Germany

Received September 3, 1997; in revised form January 27, 1998; accepted February 4, 1998

The 12 title compounds have been prepared by arc-melting cold-pressed pellets of the elemental components and subsequent annealing. They crystallize with an orthorhombic structure and with cell dimensions varying between $a = 403.9(1)$ pm, $b = 1688.4(2)$ pm, and $c = 450.6(1)$ pm for $La_3Si_2C_2$ and $a = 379.6(1)$ pm, $b = 1532.8(2)$ pm, and $c = 414.5(1)$ pm for $Tm_3Si_2C_2$. The magnetic properties of these compounds were determined with a SQUID magnetometer between 2 and 300 K with magnetic flux densities up to 5.5 T. $Y_3Si_2C_2$ is a Pauli paramagnet. The cerium atoms in $Ce_3Si_2C_2$ are trivalent; at low temperatures this compound is ferro- or ferrimagnetic with an ordering temperature of 10(±3) K. $Pr_3Si_2C_2$ and $Nd_3Si_2C_2$ are ferromagnetic ($T_C = 25(\pm3)$ and 30(±3) K, respectively), whereas the silicide carbides $R_3Si_2C_2$ with R = Sm and Gd–Tm are antiferromagnetic. $Ho_3Si_2C_2$, $Er_3Si_2C_2$, and $Tm_3Si_2C_2$ show metamagnetic transitions. The highest ordering temperature occurs for $Gd_3Si_2C_2$ with a Néel temperature $T_N = 50(\pm1)$ K. The electrical conductivities of several compounds were determined between 5 and 300 K. They indicate metallic behavior, and in several cases they reflect the magnetic ordering temperatures.

INTRODUCTION

The ternary systems of the rare earth elements with silicon and carbon have only been investigated for compositions with low carbon content. Mayer and Shidlovsky (1) reported the series R_5Si_3C (R = Y, Nd, Sm, Gd–Lu) to crystallize with a "filled" Mn_5Si_3 (Mo_5Si_3C) type structure, also known as the Nowotny phase (2). Al-Shahery, McColm, and co-workers (3–7) investigated similar compositions and found several compounds with closely related structures. We have recently reported on the crystal structure and magnetic properties of $U_3Si_2C_2$ (8). In searching for corresponding compounds with the rare earth elements, we found the compounds $R_3Si_2C_2$, which are the subject of the present investigation. They crystallize with a common orthorhombic subcell and with at least two different superstructures, which will be described in a subsequent publication (9). In the present paper we report the cell dimensions of the very pronounced subcell of this new series of rare earth silicide carbides and their magnetic and electrical properties. Some preliminary results of this work have been presented at a conference (10).

[1] To whom correspondence should be addressed.

SAMPLE PREPARATION, PROPERTIES, AND LATTICE CONSTANTS

The samples were prepared by arc-melting small (~500 mg) cold-pressed pellets of the elemental components (silicon powder: Fluka, 99.9%; graphite flakes: Alfa, >99.5%, 20 mesh). The rare earth elements were purchased in the form of ingots (>99.9%). Filings of these were prepared under dry (Na) paraffin oil, which was washed out with dry hexane. The filings were stored under vacuum and were only briefly exposed to air prior to the reactions. Samples of the ideal composition were melted in an atmosphere of purified argon twice from both sides to enhance their homogeneity. They were then wrapped in tantalum foil, annealed in evacuated silica tubes for 30 days at 900°C, and quenched in air.

The ternary carbides are all stable in air for long periods of time. Well-crystallized samples have a light gray color with metallic luster; the powders are dark gray. Energy-dispersive analyses of the samples in a scanning electron microscope were in agreement with the ideal composition and did not reveal any impurity elements heavier than sodium.

Guinier powder diagrams of the samples were recorded with Cu$K\alpha_1$ radiation and α-quartz ($a = 491.30$ pm, $c = 540.46$ pm) as an internal standard. All of the ternary $R_3Si_2C_2$ compounds crystallize with an orthorhombic structure of the space group *Cmmm* (No. 65). The cell dimensions, obtained by least-squares fits, are listed in Table 1.

0022-4596/98 $25.00

TABLE 1
Lattice Constants of Carbides with the Orthorhombic $Pr_3Si_2C_2$-Type Structure[a]

Compound	a (pm)	b (pm)	c (pm)	V (nm^3)
$Y_3Si_2C_2$	384.6(1)	1563.4(2)	421.3(1)	0.2533
$La_3Si_2C_2$	403.9(1)	1688.4(2)	450.6(1)	0.3073
$Ce_3Si_2C_2$	399.0(1)	1659.2(3)	443.4(1)	0.2935
$Pr_3Si_2C_2$	396.7(1)	1645.2(3)	439.9(1)	0.2871
$Nd_3Si_2C_2$	394.9(1)	1630.3(2)	437.5(1)	0.2817
$Sm_3Si_2C_2$	391.3(1)	1607.3(2)	431.6(1)	0.2714
$Gd_3Si_2C_2$	388.6(1)	1586.3(2)	427.6(1)	0.2636
$Tb_3Si_2C_2$	385.4(1)	1570.2(3)	423.6(1)	0.2563
$Dy_3Si_2C_2$	383.8(1)	1561.1(3)	420.3(1)	0.2518
$Ho_3Si_2C_2$	382.8(1)	1550.7(2)	418.9(1)	0.2487
$Er_3Si_2C_2$	381.1(1)	1542.0(3)	417.2(1)	0.2452
$Tm_3Si_2C_2$	379.6(1)	1532.8(2)	414.5(1)	0.2412

[a] Standard deviations in the positions of the least significant digits are given in parentheses throughout the paper.

Single-crystal investigations (9) revealed two orthorhombic superstructures with doubled a and c axes, respectively. However, the superstructure reflections are barely visible on the Guinier powder diagrams and sometimes they cannot even be detected on the precession films of single crystals. Thus, the subcell is very pronounced and it is sufficient for the unambiguous characterization of these carbides. As an example for the powder data, the evaluation of the powder diagram of $Pr_3Si_2C_2$ is shown in Table 2. No superstructure reflections were detected in this diagram. For the calculation of the intensities (11) the positional parameters as obtained for the subcell of this compound through the single-crystal investigation (9) were used.

TABLE 2
Evaluation of the Guinier Powder Diagram of $Pr_3Si_2C_2$ Recorded with Cu$K\alpha_1$ Radiation[a]

h	k	l	d_O (Å)	Q_C	Q_O	I_C	I_O
0	0	1	4.407	517	515	7	m
0	2	1	3.884	665	663	27	m
1	3	0	3.216	968	967	76	s
0	4	1	3.006	1108	1107	62	s
1	1	1	2.901	1189	1188	100	vs
0	6	0	2.742	1330	1330	38	s
1	3	1	2.596	1485	1484	22	s
1	5	0	2.533	1559	1559	7	m
0	6	1	2.328	1847	1845	4	w
0	0	2	2.202	2067	2063	24	m
1	5	1	2.195	2076	2076	27	m
1	7	0	2.022	2446	2447	5	vw
2	0	0	1.984	2542	2541	20	m
1	7	1	1.837	2963	2962	31	m
1	3	2	1.815	3035	3035	31	m
2	2	1	1.766	3206	3205	8	vw
0	6	2	1.716	3397	3397	16	w
1	5	2		3626		3	vw
1	9	0	1.660	3628	3628	14	vw
2	4	1	1.655	3650	3651	26	w
2	6	0	1.607	3872	3870	16	w
0	10	1	1.540	4211	4215	17	w
1	7	2		4513		5	vw
2	0	2	1.473	4609	4610	16	w

[a] All observed reflections and all reflections with calculated intensities $I_C > 3$ are listed; $Q = 10000/d^2$.

ELECTRICAL RESISTIVITIES

The electrical conductivity behavior of several $R_3Si_2C_2$ silicide carbides was determined with an a.c. four-probe technique (12) in the temperature range between 4 and 300 K. Compact polycrystalline pieces of 1- to 2-mm diameter selected from the crushed, arc-melted ingots were contacted with copper filaments using a silver epoxy cement. After curing at 100°C, this assembly was sealed in beeswax and slowly lowered into a Dewar flask filled with liquid helium.

The absolute values of the resistivities of the samples at room temperature varied between 100 and 270 μΩ cm. These values are estimated to be correct only within a factor of ±1.5 because of the difficulties in estimating the sizes of the contacted areas of the samples. Thus, these resistivities are slightly higher than those of the rare earth metals, e.g., yttrium with 57 μΩ cm, cerium with 75 μΩ cm, or gadolinium with 140 μΩ cm (13). The resistivities decrease with decreasing temperature (Fig. 1), as is typical for metallic conductors. At low temperatures they reflect the magnetic order; this is discussed further later.

MAGNETIC PROPERTIES

The magnetic susceptibilities of polycrystalline samples were measured in the temperature range between 2 and 300 K with magnetic flux densities up to 5.5 T using a SQUID magnetometer (Quantum Design, MPMS). Depending on the expected magnetic moments, between 8 and 20 mg of the powdered samples was filled in silica tubes of 2-mm inner diameter. The powders were held in place by compression with a cotton plug. The samples were cooled in zero field and the susceptibilities were recorded continuously at the desired magnetic flux density on heating. Usually these measurements were carried out at 0.1, 1, 3, and 5 T to reveal the general behavior of the sample and to check for ferromagnetic impurities. Minor amounts of such impurities —possibly introduced during the preparation of the filings of the rare earth components—were detected in several samples; however, in all cases the susceptibilities recorded at 3 and 5 T were practically the same and no extrapolations to infinite magnetic flux densities were necessary.

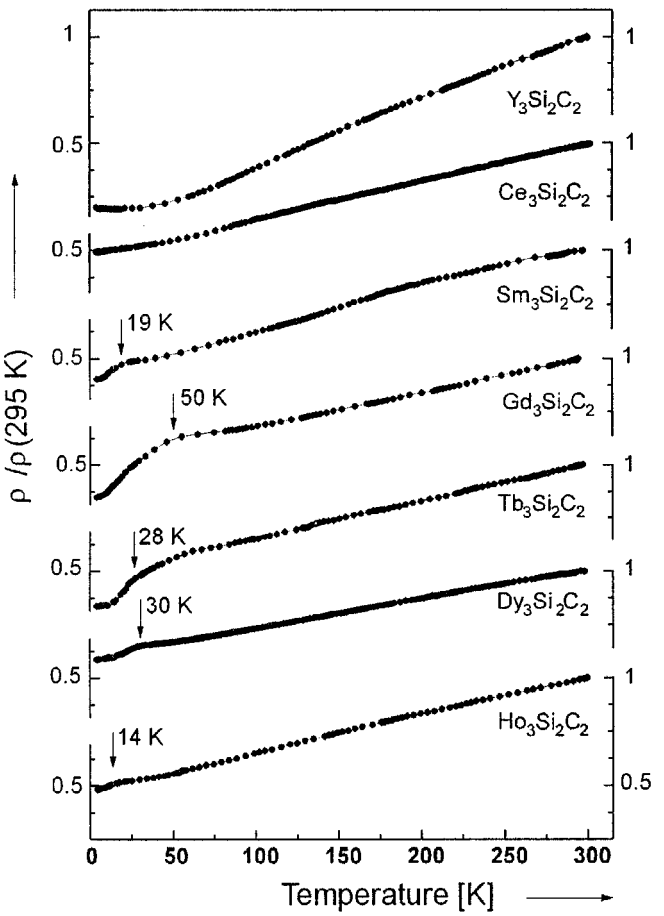

FIG. 1. Relative electrical resistivities of several rare earth silicide carbides $R_3Si_2C_2$ as a function of temperature.

The reciprocal magnetic susceptibilities of most compounds showed Curie–Weiss behavior (Fig. 2). The magnetic moments obtained from the straight portions of the $1/\chi$ vs T plots are listed in Table 3. The compounds $Pr_3Si_2C_2$, $Nd_3Si_2C_2$, and possibly also $Ce_3Si_2C_2$ were found to be ferromagnetic, whereas metamagnetic behavior was observed for $Ho_3Si_2C_2$, $Er_3Si_2C_2$, and $Tm_3Si_2C_2$. For these compounds magnetization isotherms were recorded at low temperatures (Fig. 3).

DISCUSSION

The 12 new ternary rare earth silicide carbides $R_3Si_2C_2$ are represented in Fig. 4 by the cell volumes of their orthorhombic subcells. This plot reflects the lanthanoid contraction. We have not yet been successful in preparing the corresponding compounds with europium, ytterbium, or lutetium. The cell volume of the yttrium compound fits between the cell volumes of the terbium and dysprosium compounds, as is frequently observed (14).

The magnetic susceptibility of $Y_3Si_2C_2$ is low and only very weakly temperature dependent. In view of the metallic conductivity observed for all compounds $R_3Si_2C_2$ investigated (Fig. 1), we ascribe Pauli paramagnetism to this compound. The upturn of the magnetic susceptibilities below 10 K may be due to a paramagnetic impurity. We have fitted the susceptibility values above 20 K to the modified Curie–Weiss law $\chi = \chi_0 + C(T - \Theta)^{-1}$. This resulted in $\chi_0 = 0.3 \times 10^{-9}$ m^3/mol for the temperature-independent term. This value is lower than the value of $\chi = 0.9 \times 10^{-9}$ m^3/mol measured at room temperature. However, since neither value was corrected for the core diamagnetism of the compound, the Pauli paramagnetism of $Y_3Si_2C_2$ is greater than at least the smaller of these values.

The magnetic behavior of the other silicide carbides $R_3Si_2C_2$ is dominated by the magnetism of the rare earth moments. It can be seen from the $1/\chi$ vs T plots (Fig. 2) that—with the exception of $Sm_3Si_2C_2$—all compounds follow the Curie–Weiss law. The magnetic moments calculated from the slopes of the linear portions of these plots above 100 K compare well with the theoretical ones (Table 3) for the R^{3+} ions. This is also true for the cerium compound; therefore cerium is trivalent in these compounds, as is also indicated by the volume plot. For a Ce^{4+} compound no magnetic moment and a smaller cell volume are to be expected. The magnetization curve of $Ce_3Si_2C_2$ (Fig. 3) is that of a very soft ferromagnet. The small hysteresis of this curve is due to the fact that this curve was recorded at 5 K, relatively close to the Curie temperature of $T_C = 10(\pm 3)$ K. This latter value was estimated from the turning point of the temperature dependence of the magnetization (not shown). The negative Weiss constant $\Theta = -5(\pm 2)$ K suggests complex magnetic order, possibly ferrimagnetism.

$Pr_3Si_2C_2$ and $Nd_3Si_2C_2$ are ferromagnets with Curie temperatures (again determined from the turning points of magnetization vs temperature plots) of $25(\pm 3)$ and $30(\pm 3)$ K and with positive Weiss constants (Table 3), as is normally expected for ferromagnets. Both compounds show normal hysteresis loops (Fig. 3). The saturation magnetizations $\mu_{exp(sm)} = 4.76$ μ_B/fu and $\mu_{exp(sm)} = 4.77$ μ_B/fu for $Pr_3Si_2C_2$ and $Nd_3Si_2C_2$ are considerably smaller than the highest attainable ones of 9.60 and 9.81 μ_B/fu; however, this is not unusual for powder samples, with random orientation of the easy axes of magnetization or even some preferred orientation of the crystallites with some preference of the easy axes for an orientation perpendicular to the applied field.

The Sm^{3+} ions are known to exhibit Van Vleck paramagnetism. This is also evident from the curved $1/\chi$ vs T plot of $Sm_3Si_2C_2$ above 50 K. The magnetic moment of this compound at room temperature $\mu_{exp} = 1.55(\pm 0.02)$ μ_B/Sm^{3+} calculated with the formula $\mu_{exp} = 2.83\ [(\chi_{cgs}/3)T]^{1/2}$ μ_B/Sm^{3+} is in good agreement with the value of $\mu_{eff} = 1.55$ μ_B calculated by Van Vleck (15) for Sm^{3+} at 293 K with

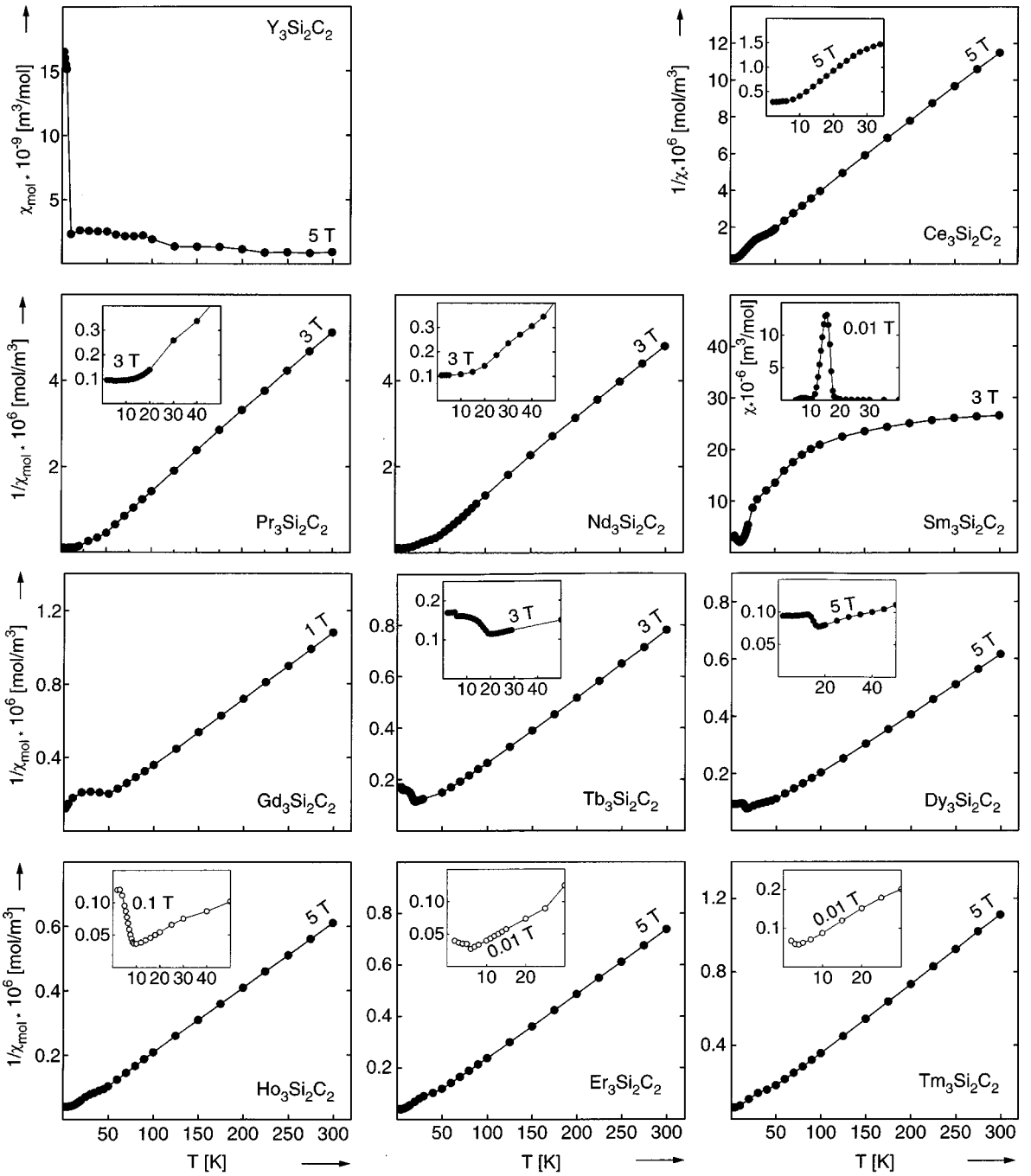

FIG. 2. Magnetic susceptibility χ of the Pauli paramagnet $Y_3Si_2C_2$ and the reciprocal susceptibilities of other carbides $R_3Si_2C_2$ (R = Ce–Nd, Sm, Gd–Tm), measured with differing magnetic flux densities (T) as indicated. The insets show the reciprocal susceptibilities at low temperatures recorded with the indicated magnetic flux densities, with the exception of the inset in the diagram of $Sm_3Si_2C_2$, where the susceptibility χ is plotted.

a screening constant of $\sigma = 33$. At low temperature the $1/\chi$ vs T plot (recorded at 3 T) has a minimum, indicating antiferromagnetic order. This minimum becomes much more pronounced when these curves are recorded with lower magnetic flux densities as can be judged from the peak of the χ vs T plot shown in the inset for this compound in Fig. 2. The peak corresponds to a Néel temperature of $16(\pm 1)$ K. This ordering temperature is also reflected in the electrical resistivity curve of this compound (Fig. 1) with an onset at $19(\pm 3)$ K.

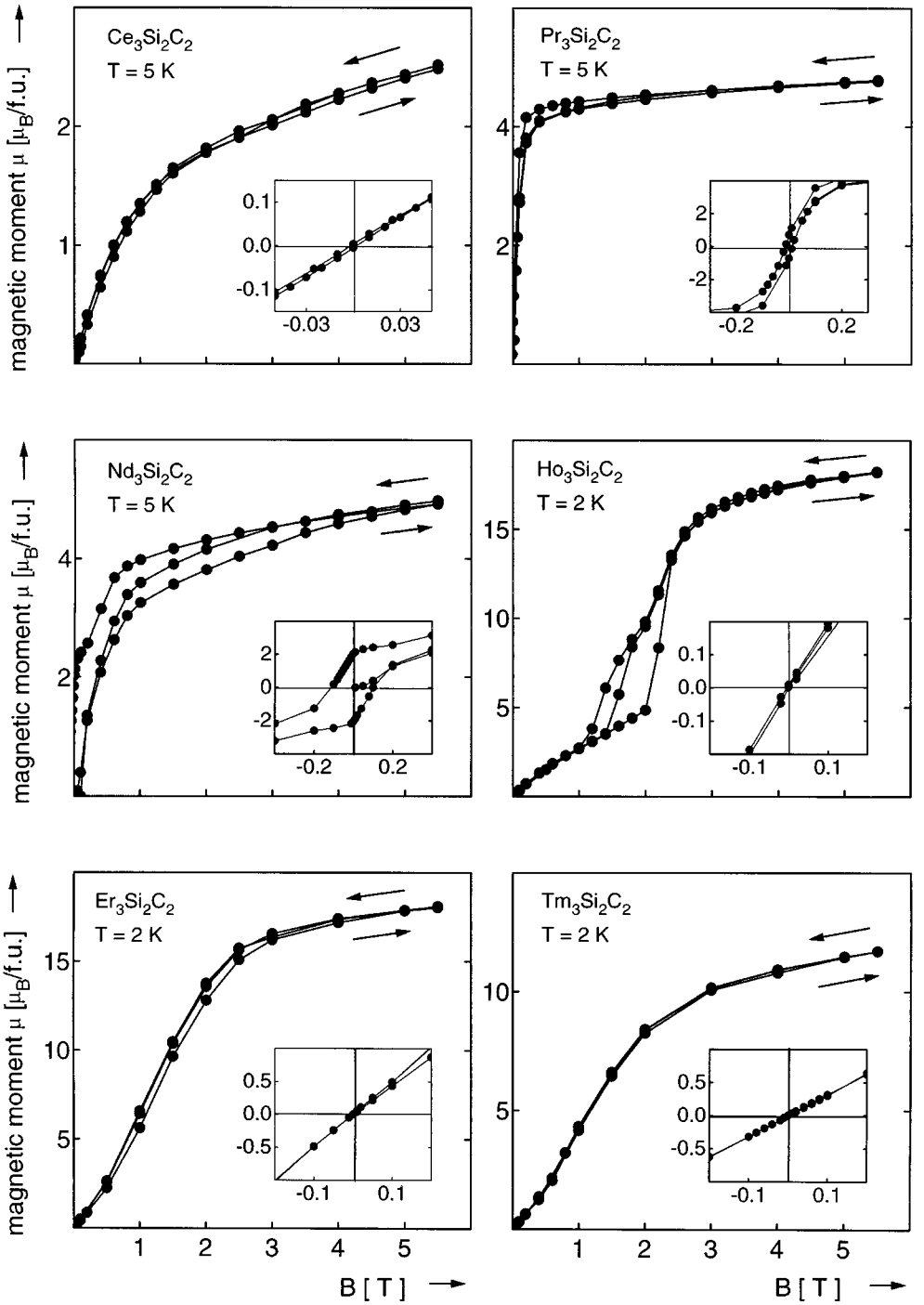

FIG. 3. Magnetization isotherms of the carbides $R_3Si_2C_2$ measured at a temperature of 2 or 5 K, respectively. The insets show the behavior of the magnetic moments at low flux densities. In the diagrams where three curves are visible, the initial (virgin) curve is also shown.

At low temperatures the $1/\chi$ vs T plots of $Gd_3Si_2C_2$, $Tb_3Si_2C_2$, and $Dy_3Si_2C_2$ show upturns indicating antiferromagnetic order with Néel temperatures of $50(\pm 1)$, $23(\pm 2)$, and $18(\pm 2)$ K, respectively. This was confirmed by the linear plots (not shown) of the magnetization vs magnetic flux density for these three compounds.

The temperature dependence of the reciprocal susceptibilities of $Ho_3Si_2C_2$, $Er_3Si_2C_2$, and $Tm_3Si_2C_2$ (Fig. 2) also suggested antiferromagnetism; however, these susceptibilities became field dependent at low temperatures, as is typical for metamagnets. This was confirmed by the magnetization measurements shown in Fig. 3. Only very little

TABLE 3
Magnetic Properties of the Carbides $R_3Si_2C_2$[a]

Compound	Magnetic behaviour	μ_{exp} $(\mu_B)/R^{3+}$	μ_{eff} $(\mu_B)/R^{3+}$	Θ (K)	$T_{C/N}$ (magn) (K)	T_N (ec) (K)	$\mu_{exp(sm)}$ (μ_B)/fu	$\mu_{calc(sm)}$ (μ_B)/fu
$Y_3Si_2C_2$	Pauli paramagnetic							
$Ce_3Si_2C_2$	Ferro- or ferrimagnetic	2.39(2)	2.54	−5(2)	10(3)		2.52	6.42
$Pr_3Si_2C_2$	Ferromagnetic	3.40(3)	3.58	21(2)	25(3)		4.76	9.60
$Nd_3Si_2C_2$	Ferromagnetic	3.53(3)	3.62	18(2)	30(3)		4.77	9.81
$Sm_3Si_2C_2$	Antiferromagnetic	1.55(2)[b]	1.55[b]	0(2)	16(1)	19(3)		
$Gd_3Si_2C_2$	Antiferromagnetic	7.69(3)	7.94	1(2)	50(1)	50(6)		
$Tb_3Si_2C_2$	Antiferromagnetic	9.01(3)	9.72	2(2)	23(2)	28(5)		
$Dy_3Si_2C_2$	Antiferromagnetic	10.12(4)	10.65	3(2)	18(2)	30(5)		
$Ho_3Si_2C_2$	Metamagnetic	10.28(4)	10.61	−4(2)	10(2)	14(5)	18.18	30.00
$Er_3Si_2C_2$	Metamagnetic	9.2(4)	9.58	7(2)	6(2)		18.06	27.00
$Tm_3Si_2C_2$	Metamagnetic	7.48(4)	7.5	7(2)	4(3)		11.69	21.00

[a] The experimentally determined paramagnetic moments μ_{exp} obtained from $\mu_{exp} = 2.83[(\chi_{cgs}/3)(T - \Theta)]^{1/2}\mu_B$ are compared with the theoretical values $\mu_{eff} = g[J(J+1)]^{1/2}\mu_B$. The highest magnetic moments $\mu_{exp(sm)}$ reached in the magnetically ordered range (at 2 or 5 K) of the powder samples are listed together with the theoretical saturation magnetizations $\mu_{calc(sm)}$ of the Ln^{3+} ions (×3), where $\mu_{calc(sm)} = 3gJ\,\mu_B$/fu. The Weiss constants Θ, the Curie temperatures T_C, and the Néel temperatures T_N found with the SQUID magnetometer (magn) or concluded from discontinuities of the electrical conductivities (ec) are also listed.

[b] The experimentally determined and the theoretical magnetic moments μ_{exp} and μ_{eff} of the samarium compound were calculated according to Van Vleck (15).

hysteresis is shown in that plot for $Er_3Si_2C_2$ and none for $Tm_3Si_2C_2$, because these curves were recorded at a temperature of 2 K, which is very close to the Néel temperatures of 6(±2) and 4(±2) K, respectively.

The magnetic ordering temperatures of $Gd_3Si_2C_2$, $Tb_3Si_2C_2$, $Dy_3Si_2C_2$, and $Ho_3Si_2C_2$ are reflected in the plots of the electrical resistivities as was discussed earlier for $Sm_3Si_2C_2$. The arrows in Fig. 1 indicate the onsets of the discontinuities estimated by us from plots with a better resolution. In almost all cases the onsets in the resistivity curves T_N(ec) are higher than the ordering temperatures found with the SQUID magnetometer $T_{C/N}$(magn) as can be seen by comparing these values in Table 3.

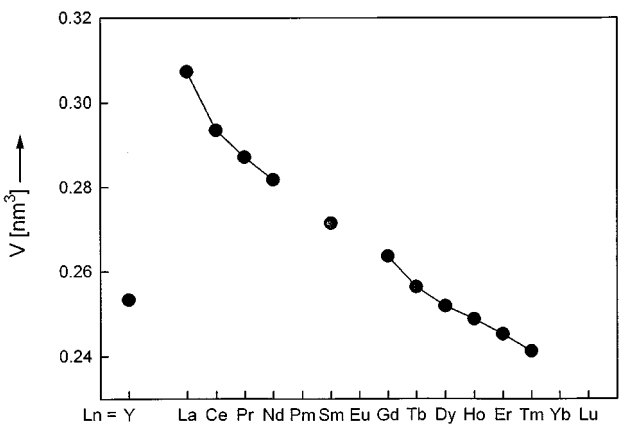

FIG. 4. Cell volumes of the carbides $R_3Si_2C_2$.

ACKNOWLEDGMENTS

We thank Mr. K. Wagner for investigating our samples in the scanning electron microscope. We are grateful to Dr. G. Höfer (Heraeus Quarzschmelze) and the Rhône-Poulenc Co. for generous gifts of silica tubes and rare earth metals. This work was also supported by the Deutsche Forschungsgemeinschaft and the Fonds der Chemischen Industrie.

REFERENCES

1. I. Mayer and I. Shidlovsky, *Inorg. Chem.* **8,** 1240 (1969).
2. E. Parthé, W. Jeitschko, and V. Sadagopan, *Acta Crystallogr.* **19,** 1031 (1965).
3. G. Y. M. Al-Shahery, D. W. Jones, I. J. McColm, and R. Steadman, *J. Less-Common Met.* **85,** 233 (1982).
4. G. Y. M. Al-Shahery, D. W. Jones, I. J. McColm, and R. Steadman, *J. Less-Common Met.* **87,** 99 (1982).
5. G. Y. M. Al-Shahery, R. Steadman, and I. J. McColm, *J. Less-Common Met.* **92,** 329 (1983).
6. T. W. Button and I. J. McColm, *J. Less-Common Met.* **97,** 237 (1984).
7. G. Y. M. Al-Shahery and I. J. McColm, *J. Less-Common Met.* **98,** L5 (1984).
8. R. Pöttgen, D. Kaczorowski, and W. Jeitschko, *J. Mater. Chem.* **3,** 253 (1993).
9. W. Jeitschko, M. H. Gerdes, A. M. Witte, and U. Ch. Rodewald, *J. Solid State Chem.*, in preparation.
10. A. M. Witte and W. Jeitschko, *Z. Kristallogr. Suppl.* **10,** 96 (1995).
11. K. Yvon, W. Jeitschko, and E. Parthé, *J. Appl. Crystallogr.* **10,** 73 (1977).
12. L. J. van der Pauw, *Philips Res. Rep.* **13,** 1 (1958).
13. "Handbook of Chemistry and Physics" (R. C. Weast, Ed.), 57th ed. CRC Press, Cleveland, OH, 1977.
14. Th. Hüfken, A. M. Witte, and W. Jeitschko, *J. Alloys Compd.* **266,** 158 (1998).
15. J. H. Van Vleck, "The Theory of Electric and Magnetic Susceptibilities." Oxford University Press, London, 1932.